

Neutron multimonochromator-bipolarizer based on magnetic multilayer Fe/Co and new scheme for the total neutron polarization analysis

V.G. Syromyatnikov^{1,2}, Kyaw Zaw Lin¹

¹ Department of Physics, St. Petersburg State University, Ulyanovskaya, 1, Petrodvorets, St. Petersburg 198504, Russia

² Neutron Research Department, Petersburg Nuclear Physics Institute, National Research Center “Kurchatov Institute”, Orlova Roscha, Gatchina, St. Petersburg 188300, Russia

syromyatnikov_vg@npi.nrcki.ru

Abstract. In this paper, we present a new neutron-optical element, Neutron Multimonochromator-Bipolarizer (NMB). It consists of a multimultilayer structure made of 12 periodic multilayer Fe/Co magnetic nanostructures whose period increases with distance from the substrate. Results are presented of calculations of the reflection coefficients from the NMB. We propose a new scheme of the total neutron polarization analysis for the time-of-flight method in the reflectometry. In this scheme, double NMB is used as a polarizer and there is no spin-flipper before the sample. NMB can be used in polarized neutron reflectometry, in SESANS, and for research of low-angle and inelastic scattering of polarized neutrons.

1. Introduction

In recent years the number of experiments on the study of surfaces and multilayer nanostructures by neutron reflectometry has significantly increased. In recent years, the number has increased significantly of neutron-reflectometry experiments on surfaces and multilayer nanostructure. Polarized neutron reflectometry [1] plays a unique role in the study of interphase boundaries and multilayer nanostructures. The latter are used increasingly in the electronics industry and in creating unique scientific equipment such as neutron multilayer monochromators, supermirror polarizers, and analyzers.

There is a number of works devoted to multilayer periodic nanostructures consisting of alternating layers of two different materials [2-9]. There is a Bragg peak of the 1st order on a curve of a reflectivity of a neutron beam from such a nanostructure. The magnitude of this peak is proportional to the square of the difference between the neutron-optical potentials of materials of the structure. If one of these materials is magnetic and another one is nonmagnetic, such a structure with suitable characteristics of materials can serve as a neutron multilayer monochromator-polarizer. The difference between neutron-optical potentials of the layers in the saturating magnetic field can be made sufficiently great for one spin component of the beam and negligibly small for another one. As a result, the reflectivity of the Bragg peak is close to 1 and to 0, in the former and in the latter cases,



respectively (see, e.g., [8, 9]). Therefore, the beam reflected from such a structure is monochromatic and polarized.

In [10], we studied a periodic magnetic multilayer Fe / Co nanostructure. In this structure, both materials are magnetic. Parameters of materials of layers for the saturating magnetic field are presented in Table 1.

Table 1. Parameters of materials of iron and cobalt layers. Here SLD (+) and SLD (-) are Scattering Length Density for spin-up and spin-down neutrons, correspondingly; σ_{abs} is the cross-section of absorption of neutrons by nuclei of material.

Parameters	Fe	Co
d (Å)	100	110
SLD (+) (10^{10} cm^{-2})	13.13	6.45
SLD (-) (10^{10} cm^{-2})	2.93	-1.98
σ_{abs} (10^{-24} cm^2)	2.56	37.18

A structure consisting of 20 pairs of alternating layers was created on a polished glass substrate. Thicknesses of the iron and cobalt layers were 100 Å and 110 Å, respectively. Reflection coefficients for (+) and (-) spin components of the neutron beam as a function of the momentum transfer were measured in such nanostructure for several values of the in-plane external magnetic field. Measurements were carried out using the time-of-flight method on neutron reflectometer NR-4M [11] (the reactor WWR-M PNPI NRC “KI”). The corresponding experimental data and theoretically obtained curves (solid lines) are shown in Fig. 1 for the saturating magnetic field $H = 472$ Oe [10]. The value of the reflectivity smaller than one below the critical edge and low values of the Bragg reflections of the 1st order are due to the absorption in cobalt layers and the roughness of the layers. The roughness of layers was 35 Å.

It follows from Fig. 1 that intensities of Bragg peaks of the 1st order are close for (+) and (-) spin component but their positions are shifted relative to one another. Furthermore, it was also found that intensities of these Bragg peaks are weakly dependent on the magnetic field. These unusual properties of Fe / Co nanostructures can be explained by the fact that differences are significant between the neutron optical potentials of iron and cobalt layers for (+) and (-) spin components of the beam [10]. Let us consider this point in more detail. As it is well known, in the kinematic approximation, the reflection coefficient of the Bragg peak of the 1st order of the multilayer monochromator-polarizer consisting of alternating layers of two kinds of materials depends, in particular, on the square of the difference between scattering length densities of adjacent layers [4]. It appears that this difference is slightly dependent on the magnetic field applied to the Fe / Co structure [10]. Therefore, Bragg peaks of the 1st order are virtually independent of the applied magnetic field in the (ideal) Fe / Co structure.

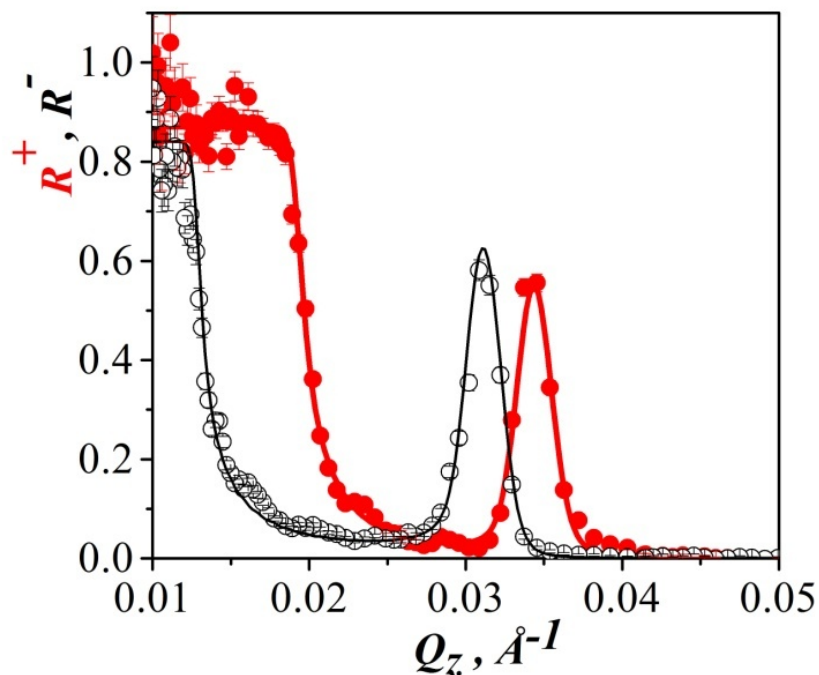


Figure 1. Reflection coefficients of both spin components of the neutron beam as a function of the normal component of the momentum transfer Q_z for the scattering from the multilayer periodic magnetic nanostructure Fe / Co. Experimental data and results of theoretical calculations (solid lines) are shown for the saturating in-plane magnetic field $H = 472$ Oe.

2. Calculations of the neutron multimonochromator-bipolarizer

After analysis of experimental results for the multilayer periodic magnetic Fe / Co nanostructures [10], one of the authors of the present work (V.S.) suggested to use these unique properties of Fe / Co nanostructures to polarize and monochromize a neutron beam with opposite polarizations for two close monochromatic wavelengths. In this case, measurements of intensities I^+ and I^- reflected from the sample can be obtained without the spin flipper. If one uses a set of similar structures with properly chosen different periods, one measurement would give dependences of both I^+ and I^- on the momentum transfer that would reduce the time of the experiment. To realize this idea, one of the authors of the present paper (V.S.) proposed a new neutron-optical element, Neutron Multimonochromator-Bipolarizer (NMB). NMB has a multimultilayer structure that consists of twelve periodic multilayer magnetic Fe/Co nanostructures. Each periodic multilayer magnetic nanostructure has a considerable number of identical bilayers and its own thickness of the bilayer (or the period value). The structure is schematically shown in Fig. 2 of a NMB with twelve periodic magnetic Fe/Co nanostructures in which period values increase with distance from the substrate. Iron and cobalt layers in each periodic structure have the same thickness. This eliminates Bragg peaks of the 2nd order for each periodic structure. Each structure has two Bragg peaks of the 1st order on the reflectivity curve for (+) and (-) spin components with the reflection coefficients close to 1. Values of structures periods

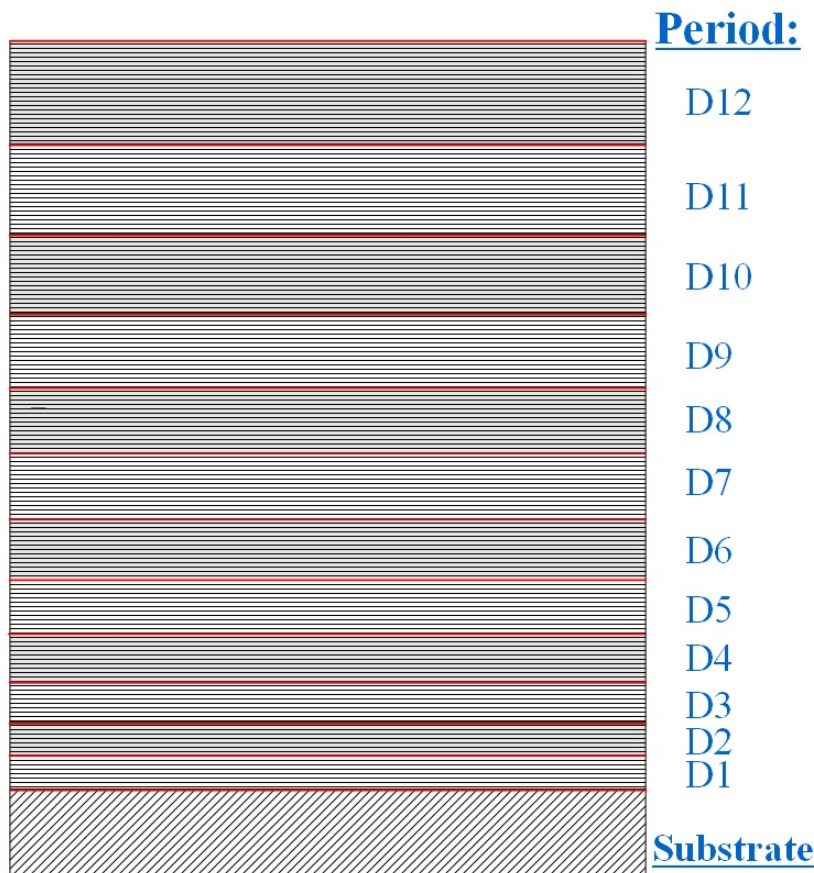


Figure 2. Scheme of multimilayer structure of NMB made of twelve periodic multilayer magnetic Fe/Co nanostructures whose periods increase with distance from the substrate.

have been selected so that the Bragg peak of the first order for (+) spin component of each structure and the Bragg peak for (-) spin component of the neighboring structure (with larger period) to be as close to each other as possible. Thus, the reflection coefficient for this NMB should show a set of densely standing alternating Bragg peaks of the 1st order.

The scheme of such NMB is presented in Fig. 3a. Schemes of distribution of neutron-optical potentials for periodic Fe/Co nanostructures in the NMB for (+) and (-) neutron spin components are presented in Figs. 3b and 3c, correspondingly. As it is seen from Figs. 3b and 3c, there is a large difference of neutron-optical potentials for both spin components of the beam for all structures in NMB. Therefore, on curves of reflectivities of both spin components from each periodic structure depending on the momentum transfer, at sufficient number of pairs of layers in each structure, almost identical Bragg peaks of first order should be observed which are slightly displaced from each other and which intensities are close to 1.

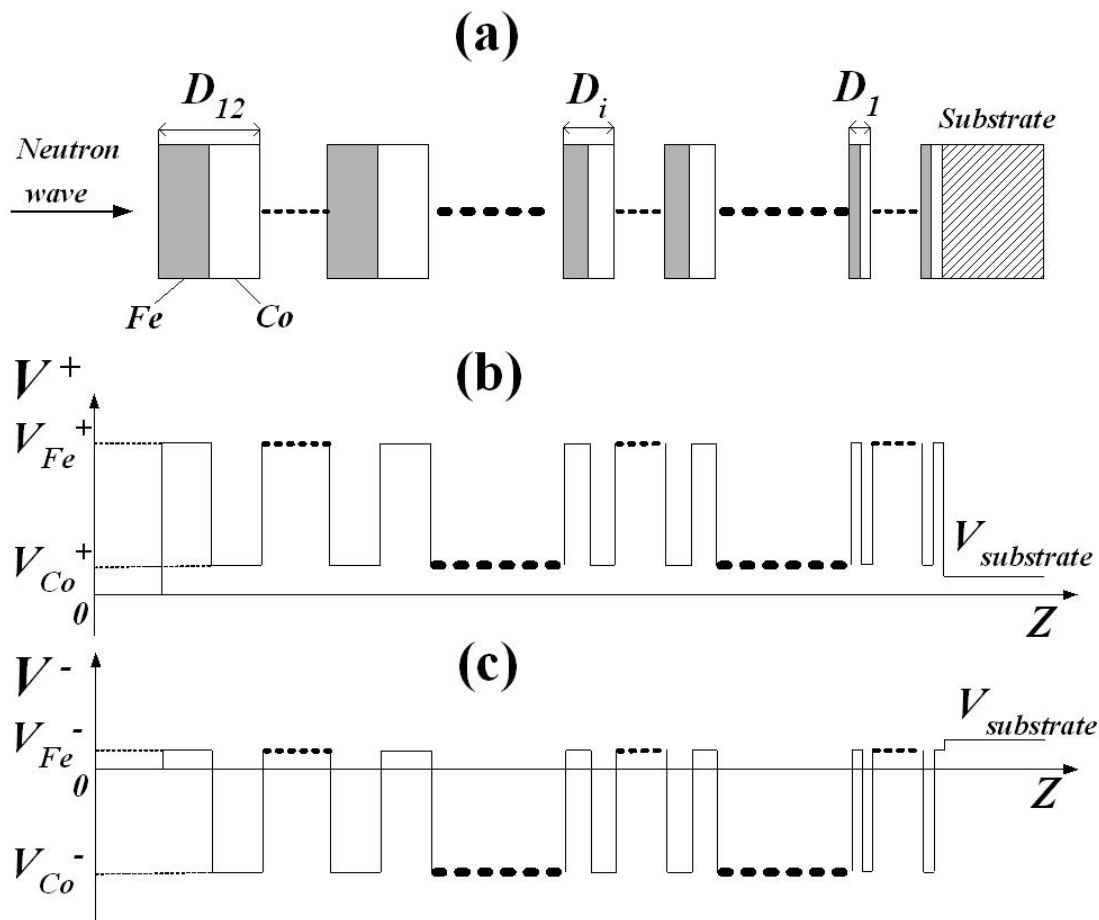


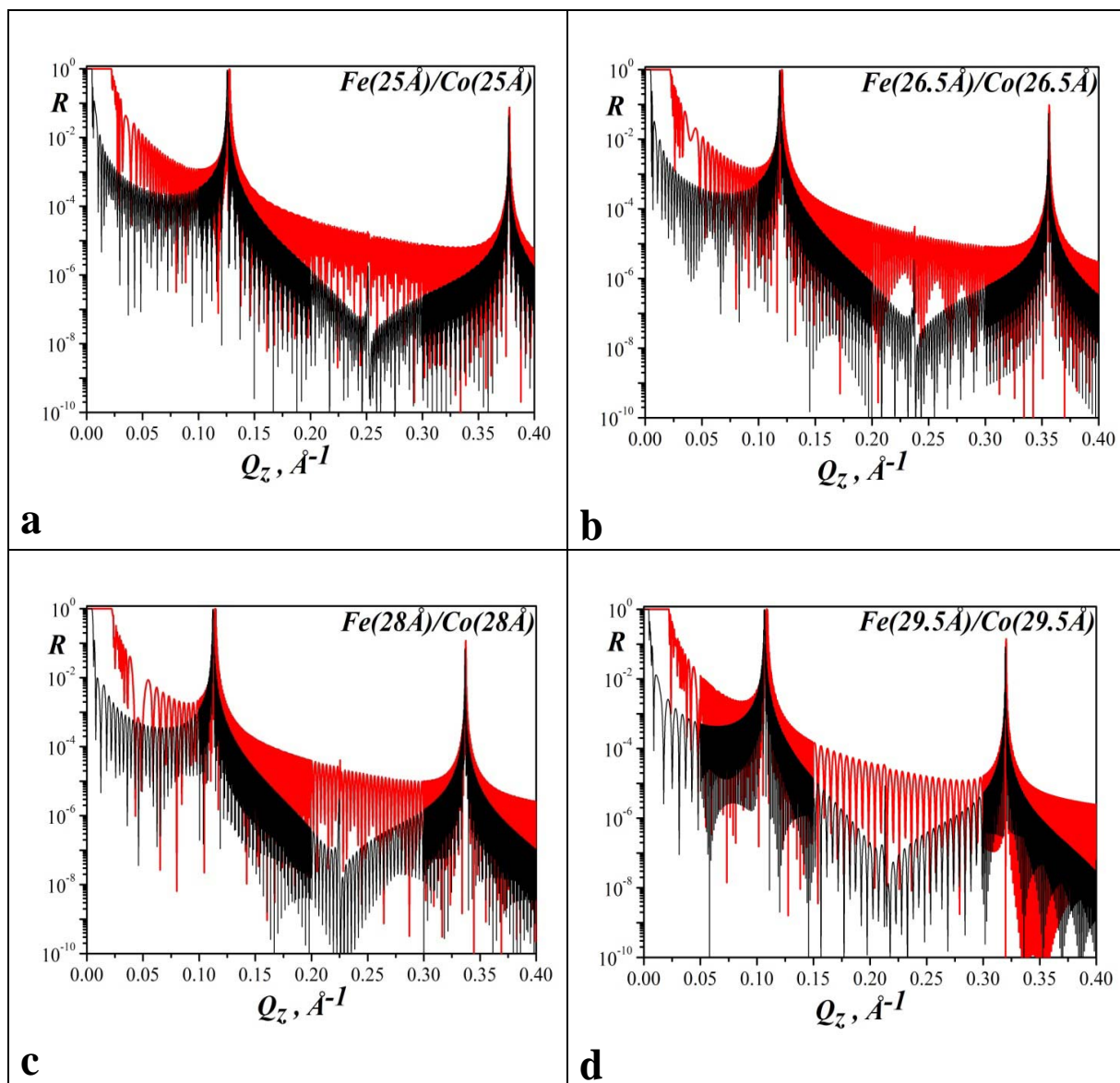
Figure 3. Scheme of periodic Fe/Co structures in NMB (a); scheme of distribution of neutron-optical potentials for periodic Fe/Co structures in NMB for (+) (b) and for (-) (c) neutron spin components.

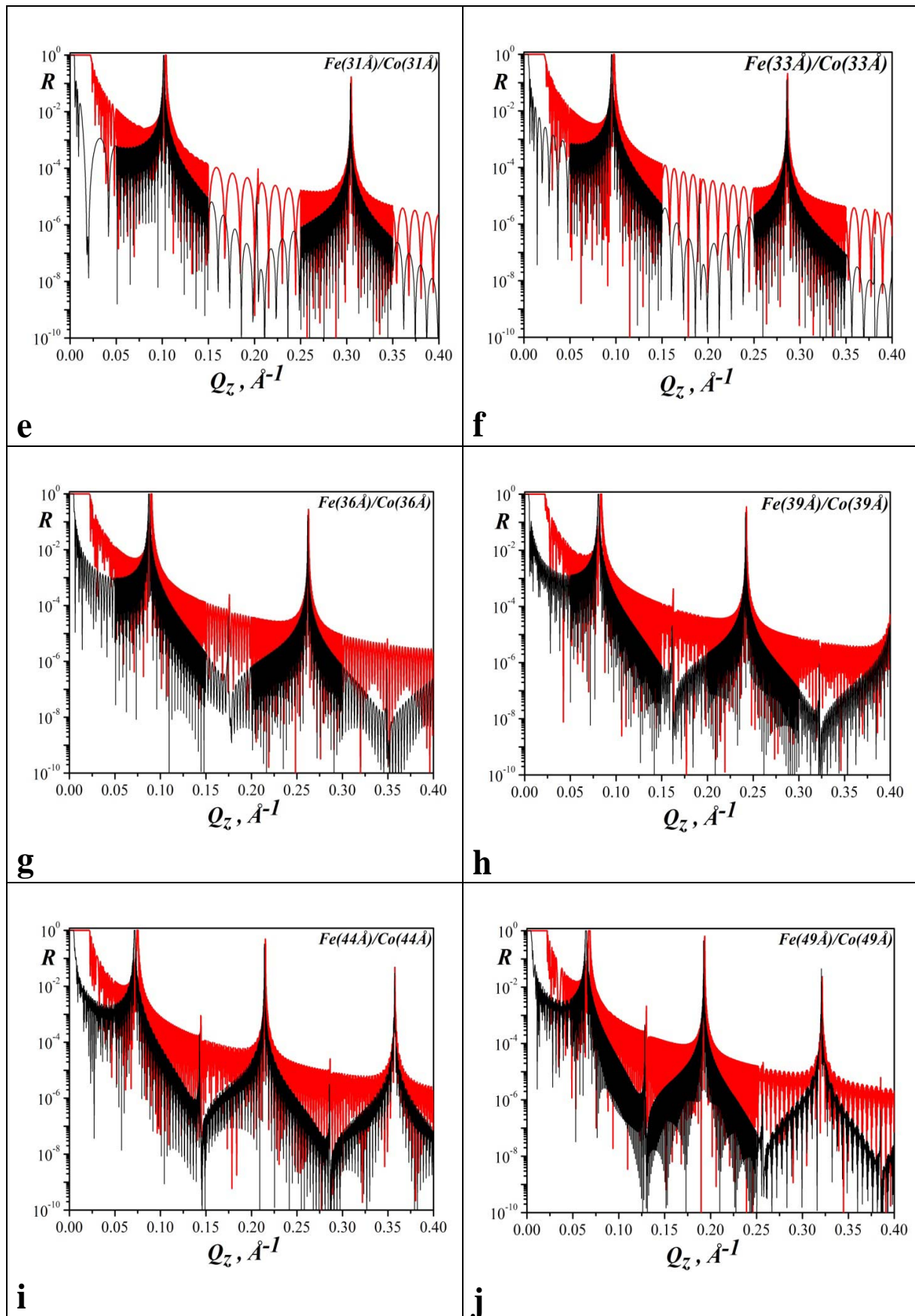
Standard Parratt32 program was used for calculations, which is one of the most effective tools for studying of multilayered nanostructures. Coefficients of reflection from each of twelve multilayer periodic magnetic nanostructures are presented in Fig. 4, which were obtained as results of calculations. The absorption of neutrons in the materials of the layers of structures was not taken into account. Periods of nanostructures in this NMB have the following values: $D_1=50 \text{ \AA}$ (a), $D_2=53 \text{ \AA}$ (b), $D_3=56 \text{ \AA}$ (c), $D_4=59 \text{ \AA}$ (d), $D_5=62 \text{ \AA}$ (e), $D_6=66 \text{ \AA}$ (f), $D_7=72 \text{ \AA}$ (g), $D_8=78 \text{ \AA}$ (h), $D_9=88 \text{ \AA}$ (i), $D_{10}=98 \text{ \AA}$ (j), $D_{11}=118 \text{ \AA}$ (k), $D_{12}=146 \text{ \AA}$ (l). Such periods provide a set of densely standing alternating Bragg peaks of the 1st order with opposite spins (see above). Each multilayered nanostructure of this NMB contains 245 bilayers. Layer thicknesses are the same in each structure. The structure with period D_1 is evaporated on the glass substrate.

As is seen from Fig. 4, only Bragg peaks of odd orders are visible in each nanostructure for both spin components of the beam. For Bragg peaks of the 1st order, coefficients of reflection are close to 1 for both spin components. The absence of peaks of even orders is explained by the fact that thicknesses of layers in every period are identical [9].

In Fig. 5, we present calculated coefficients of reflection from the NMB consisting of twelve periodic magnetic Fe/Co nanostructures with periods $D_1=50 \text{ \AA}$, $D_2=53 \text{ \AA}$, $D_3=56 \text{ \AA}$, $D_4=59 \text{ \AA}$, $D_5=62 \text{ \AA}$, $D_6=66 \text{ \AA}$, $D_7=72 \text{ \AA}$, $D_8=78 \text{ \AA}$, $D_9=88 \text{ \AA}$, $D_{10}=98 \text{ \AA}$, $D_{11}=118 \text{ \AA}$, $D_{12}=146 \text{ \AA}$. The

number of bilayers in all periodic structures remains the same and equals to 245. Calculations were carried out without taking into account a structure imperfection and the absorption of neutrons in materials of layers. These dependences show 13 pairs of peaks located close to each other, which reflection coefficients are close to 1. Red and black curves correspond to R^+ and R^- , respectively. The number of peak pairs corresponds to the number of periods of NMB. Peaks in a pair are Bragg peaks of the 1st order of the corresponding period for (+) and (-) spin components. Peaks in the thirteenth pair are Bragg peaks of the 3rd order for (+) and (-) spin components produced by the structure with period D_{12} .





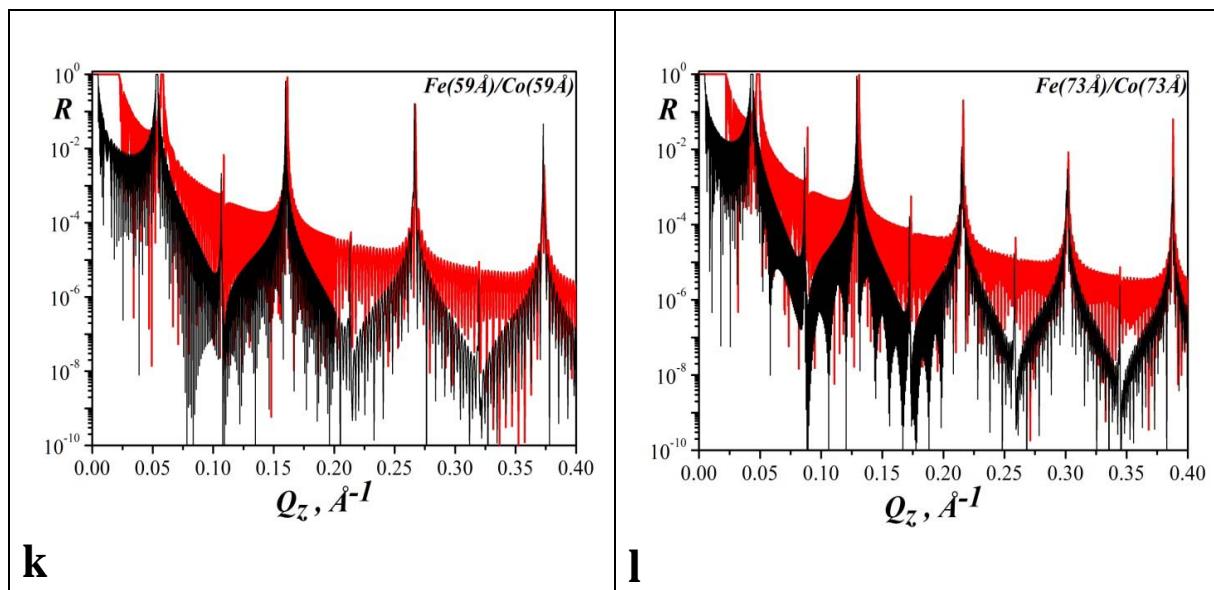


Figure 4. Calculated reflection coefficients of both spin components of the neutron beam from each of twelve multilayered periodic magnetic nanostructures as functions of the normal component of the momentum transfer. Periods of nanostructures in this NMB are $D_1=50 \text{ \AA}$ (a), $D_2=53 \text{ \AA}$ (b), $D_3=56 \text{ \AA}$ (c), $D_4=59 \text{ \AA}$ (d), $D_5=62 \text{ \AA}$ (e), $D_6=66 \text{ \AA}$ (f), $D_7=72 \text{ \AA}$ (g), $D_8=78 \text{ \AA}$ (h), $D_9=88 \text{ \AA}$ (i), $D_{10}=98 \text{ \AA}$ (j), $D_{11}=118 \text{ \AA}$ (k), $D_{12}=146 \text{ \AA}$ (l).

As appears from Fig. 5, a small overlapping occurs of peak wings of neighboring peak pairs. Let us consider this point in more detail. In Figs. 6a and 6b, we show calculated reflectivities from the nanostructure of NMB with period $D_7=72 \text{ \AA}$ near Bragg peaks of the 1st order for single (a) and double (b) reflections. Calculations were carried out without taking into account the absorption of neutrons in materials of layers. Notice that at single reflection (Fig. 6a) a small overlapping of peaks is observed, there is practically no overlapping at double reflection (Fig. 6b), whereas peaks heights are the same in both cases. Therefore, the degree of polarization of Bragg peaks for this period will be significantly higher after double reflection than after single reflection. This statement is valid also for all other structures of this NMB.

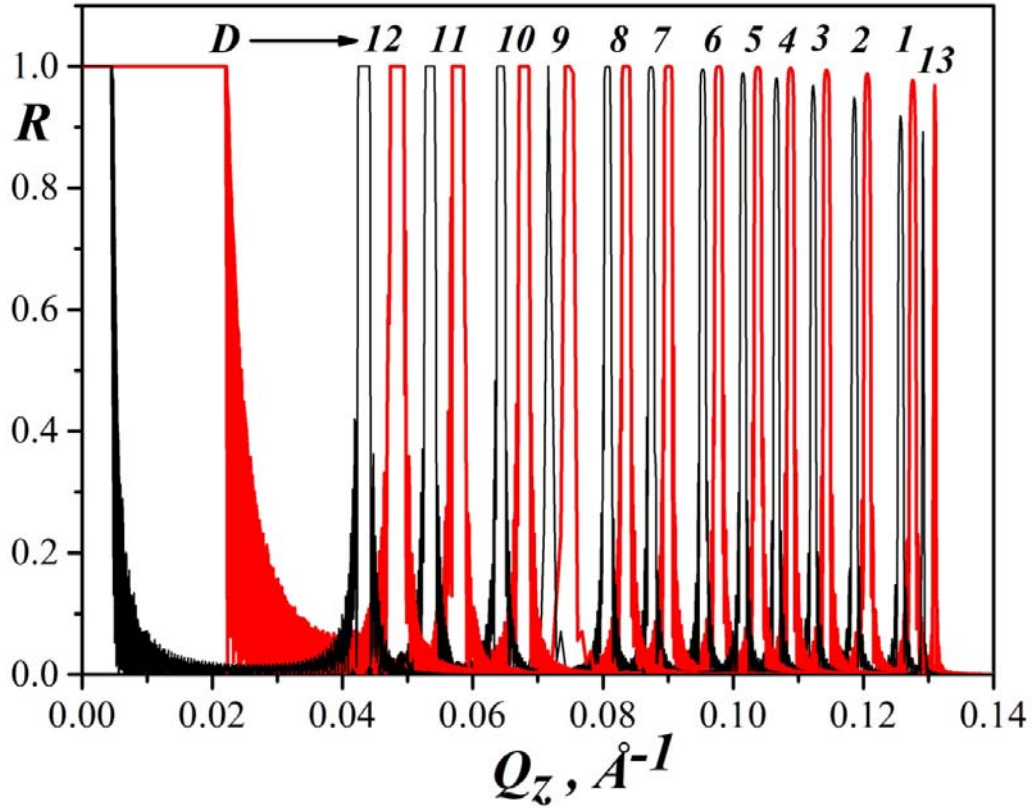


Figure 5. Calculated reflection coefficients of both spin components of the beam as functions of the normal component of the momentum transfer of the NMB consisting of twelve periodic magnetic Fe/Co nanostructures with periods $D_1=50 \text{ \AA}$, $D_2=53 \text{ \AA}$, $D_3=56 \text{ \AA}$, $D_4=59 \text{ \AA}$, $D_5=62 \text{ \AA}$, $D_6=66 \text{ \AA}$, $D_7=72 \text{ \AA}$, $D_8=78 \text{ \AA}$, $D_9=88 \text{ \AA}$, $D_{10}=98 \text{ \AA}$, $D_{11}=118 \text{ \AA}$, $D_{12}=146 \text{ \AA}$. R^+ and R^- are shown in red and black, respectively. Each of the twelve periodic Fe / Co structures contains 245 bilayers.

Parameters are presented in Table 2 of Bragg peaks of the 1st and the 3rd orders which are shown in Fig. 5.

Let us introduce coefficient of attenuation A_i of a monochromatic neutron beam when reflected from the i -th periodic structure of NMB. We define this coefficient as

$$A_i = \exp(-\gamma_i),$$

$$\text{where } \gamma_i = \frac{8 \cdot \pi \cdot \bar{N} \cdot \bar{\sigma}}{\lambda_0 \cdot Q_{zBli}} \cdot \sum_{k=i}^{12} n_k \cdot d_k, \quad 1 \leq i \leq 12,$$

where Q_{zBli} is the value of the normal component of the momentum transfer corresponding to the Bragg reflection of the 1st order from the i -th periodic structure of NMB (i is counted from the substrate), n_k is the number of bilayers in the k -th periodic structure ($k \geq i$), d_k is the thickness of bilayer in the k -th periodic structure, $\bar{N} \cdot \bar{\sigma} = (N_{Fe} \cdot \sigma_{abs Fe} + N_{Co} \cdot \sigma_{abs Co}) / 2 = 1.78 \text{ cm}^{-1}$, N_{Fe} and

N_{Co} are numbers in 1 cm^3 of iron and cobalt nuclei, respectively, $\sigma_{abs Fe}$ and $\sigma_{abs Co}$ are cross-sections of absorption of neutrons by iron and cobalt nuclei, correspondingly, and $\lambda_0 = 1.8 \text{ \AA}$.

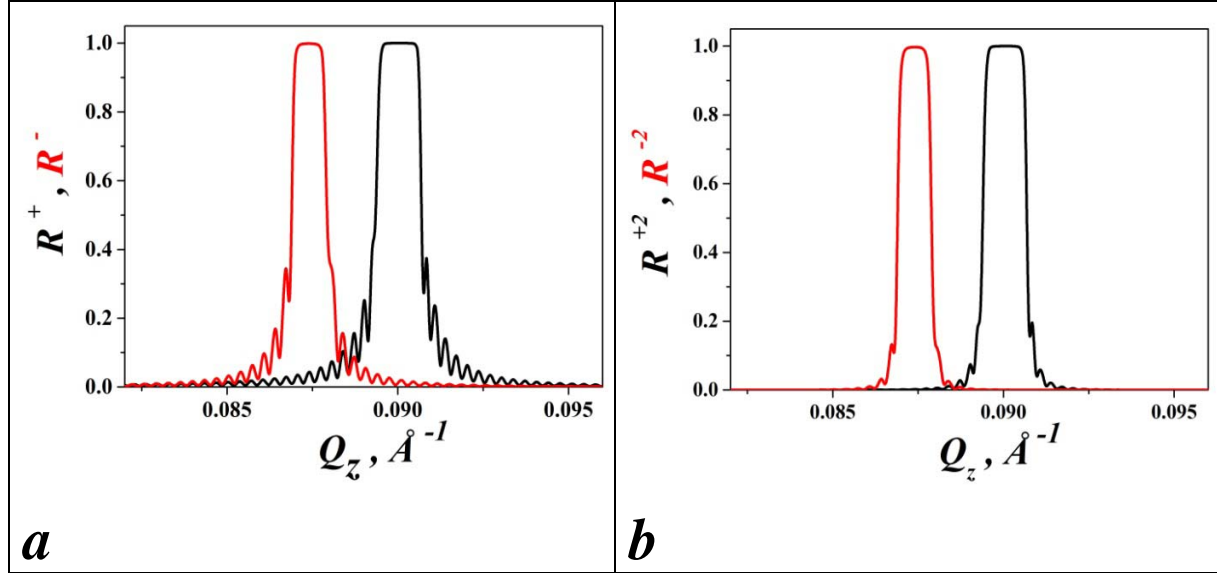


Figure 6a, b. Calculated reflectivities from the nanostructure of NMB with period $D_7 = 72 \text{ \AA}$ near Bragg peaks of the 1st order for single (a) and double (b) reflections.

Table 2. Parameters of Bragg peaks of the 1st and the 3rd orders shown in Fig. 5. Here i is the number of the periodic structure in NMB. For $i = 1, 2, \dots, 12$, parameters of Bragg peaks of the 1st order are specified for structures with periods $D_1 - D_{12}$. For $i = 13$, parameters of Bragg peaks of the 3rd order are specified for the structure with period D_{12} . d is the value of period, $R_{B1i, B313}^\pm$ are reflectivities of Bragg peaks for (+) and (-) spin components of the neutron beam, $Q_{zB1i, B313}^\pm$ are positions of Bragg peaks produced by i -th structure, $\left(\frac{\Delta Q_{zB1i, B313}}{Q_{zB1i, B313}}\right)^\pm$ are relative widths of Bragg peaks of the first and the

third orders, $P_{Q_{zB1i, B313}^\pm}$ are polarizing efficiencies of Bragg peaks of the first and the third orders given by $P_{Q_{zB1i, B313}^\pm} = [R_{B1i, B313}^+(Q_{zB1i, B313}^+) - R_{B1i, B313}^-(Q_{zB1i, B313}^+)] / [R_{B1i, B313}^+(Q_{zB1i, B313}^+) + R_{B1i, B313}^-(Q_{zB1i, B313}^+)]$; A_{1i} and A_{2i} are coefficients of attenuation of monochromatic neutron beams, when the number of bilayers in all 12 periodic structures of NMB are the same and equal to 245 and 100, respectively.

i	d (\AA)	$R_{B1i, B3}^+$	$Q_{zB1i, B3}^+$ (\AA^{-1})	$R_{B1i, B3}^-$	$Q_{zB1i, B313}^-$ (\AA^{-1})	$\left(\frac{\Delta Q_{zB1i, B313}}{Q_{zB1i, B313}}\right)^+$	$\left(\frac{\Delta Q_{zB1i, B313}}{Q_{zB1i, B313}}\right)^-$	$P_{Q_{zB1i, B313}^\pm}$	A_{1i}	A_{2i}
1	50	0.98	0.128	0.92	0.126	0.0085	0.0068	0.952	0.64	0.83
2	53	0.98	0.121	0.95	0.119	0.0099	0.0076	0.999		
3	56	0.98	0.114	0.96	0.112	0.0099	0.0081	0.951		

4	59	0.99	0.109	0.98	0.107	0.0107	0.0090	0.949		
5	62	0.99	0.104	0.99	0.102	0.0115	0.0094	0.949		
6	66	1	0.098	0.99	0.095	0.0127	0.0105	0.987		
7	72	1	0.090	1	0.087	0.0133	0.0106	0.958	0.67	0.85
8	78	1	0.084	1	0.081	0.0149	0.0114	0.987		
9	88	1	0.075	1	0.072	0.0187	0.0182	0.969		
10	98	1	0.068	1	0.064	0.0280	0.0218	0.960		
11	118	1	0.058	1	0.053	0.0308	0.0346	0.959		
12	146	1	0.048	1	0.043	0.0577	0.0462	0.959	0.83	0.93
13	146	0.97	0.131	0.89	0.129	0.0027	0.0019	0.99	0.93	0.97

As follows from Table 2, Bragg peaks of the first order for all periodic structures and Bragg peaks of the 3rd order for the structure with $N = 12$ have high reflectivities $R_{B1}^+ > 0.97$ and $R_{B1}^- > 0.89$. The relative widths of Bragg peaks are in range $(\Delta Q_{B1}/Q_{B1})^{\pm} = 0.002 - 0.058$. The polarizing efficiency for all Bragg peaks is high $P_{Q_{B1}, B3}^+ \geq 0.95$. Coefficient of attenuation A_i depends significantly on the number of bilayers in periodic structures of NMB. Then, A_{2i} is greater than A_{1i} in all considered structures. This value can be increased further by reflecting the neutron beam twice from a given NMB, as it is discussed above by the example of the structure with period $D_7 = 72 \text{ \AA}$. Thirteen pairs of Bragg peaks presented in Fig. 5 including peaks of the 3rd order cover the considerable range of the momentum transfer $Q_Z = (0.043 - 0.131) \text{ \AA}^{-1}$, where $Q_{Z \max} / Q_{Z \min} \cong 3.05$.

3. The new scheme of the total neutron polarization analysis

Four-modes neutron reflectometer NR-4M [11] at the WWR-M reactor of Petersburg Nuclear Physics Institute (PNPI NRC KI) was constructed using the traditional scheme of the total neutron polarization analysis, where the main components in the monochromatic polarization mode are monochromator-polarizer, two spin-flippers (one before and one after the sample), sample, analyzer, and detector. The scheme of neutron reflectometer NR-4M in polarization modes is shown in Fig. 7.

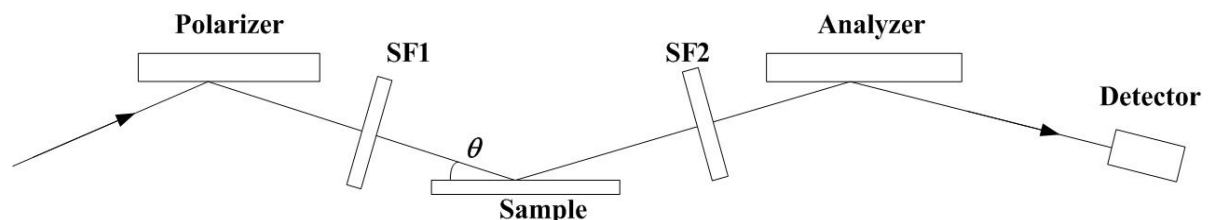


Figure 7. Scheme of neutron reflectometer NR-4M in polarization modes [11].

In the monochromatic polarization mode of neutron reflectometer NR-4M, the mirror multilayer monochromator-polarizer is used which is based on the pair Co/Ti [7]. Scheme of the double mirror monochromator-polarizer based on the Co / Ti pair is shown in Fig. 8a.

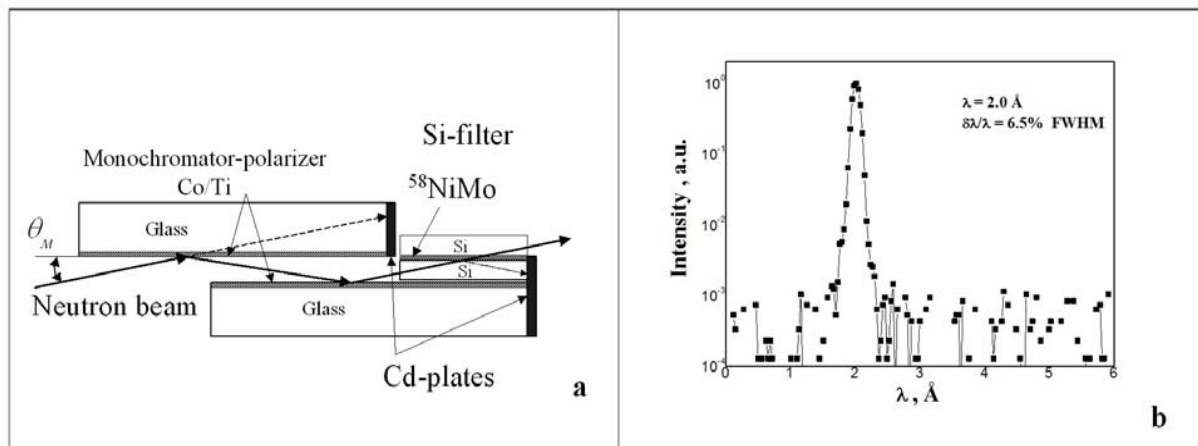


Figure 8. (a) Scheme of mirror neutron monochromator-polarizer based on Co / Ti in the unit of the beamformer of neutron reflectometer NR-4M, (b) Intensity of (+) spin component of the beam as a function of wavelength at the exit of the monochromator-polarizer after double reflection from the monochromator-polarizer and after passing of the beam through the filter.

The neutron beam with a broad spectral distribution falls on the mirror monochromator-polarizer Co / Ti at the glancing angle θ_m . Due to the Bragg diffraction on periodic Co / Ti structure [7], monochromatic neutrons are reflected from it with wavelength λ and with spins parallel to the magnetic field. Neutrons with this wavelength and with spins opposite to the magnetic field are not practically reflected. They pass through the whole structure, through the glass substrate, and they are absorbed in a cadmium plate which is glued to the substrate edge. By setting the appropriate angle θ_m , one can obtain the desired wavelength λ of the monochromatic beam passing through the unit. As is seen from Fig. 8a, the double reflection of neutrons and the silicon filter are used in the monochromator-polarizer Co / Ti. This is done in order to improve the polarization of the reflected neutron beam and to increase the degree of its monochromatization. In Fig. 8b, the dependence on the wavelength is shown of the intensity of (+) spin component of the beam at the exit of the monochromator-polarizer that is tuned to wavelength of $\lambda = 2 \text{ \AA}$. Parasitic contributions to the reflected intensity amount to only 0.2% from non-monochromatic neutrons after double reflection from the monochromator-polarizer Co / Ti and after passing through the silicon filter. The polarization of the produced monochromatic beam is very high: the flipping ratio at the peak is 250. The flipping ratio is defined as $I^+(\lambda)/I^-(\lambda)$. In Fig. 8b, only $I^+(\lambda)$ is shown. The highly polarized monochromatic beam with a wavelength λ formed thereby passes through the first collimation system, the first spin-flipper, and falls on the sample at the glancing angle θ . The reflected beam from the sample with the intensity I falls on the supermirror analyzer after passing through the second spin-flipper. The reflected beam from the analyzer is recorded by the detector. In this scheme of the total polarization analysis, four intensities (I^{++} , I^{+-} , I^{-+} , I^{--}) are measured in four measurements. Here, signs "+" and "-" correspond to situations when the spin-flipper is switch on and switch off, respectively. When the spin-flipper is switched on, the neutron spin flips. When it switched off, the beam passes through the spin-flipper without a spin flip. The first and the second signs "+" or "-" indicate the state of the first and of the second spin-flipper, correspondingly. Four values $I^{++}(Q_z)$, $I^{+-}(Q_z)$, $I^{-+}(Q_z)$, $I^{--}(Q_z)$ (where $Q_z = \frac{4\pi \sin \theta}{\lambda}$) can be measured by carrying out such measurements (the total polarization analysis) in the wide range of glancing angles θ of the beam on

the sample. It is possible to obtain a reflectivity matrix for each value of Q_z from these four intensities.

In the supermirror polarization mode of neutron reflectometer NR-4M [11], the conventional total neutron polarization analysis scheme is also used. The main set-up components are supermirror polarizer, two spin-flippers (one before and one after the sample), the sample, supermirror analyzer and detector. In Fig. 9a, we show the supermirror polarization mode of NR-4M reflectometer, in which a double polarizing CoFeV / TiZr supermirror is used as a polarizer.

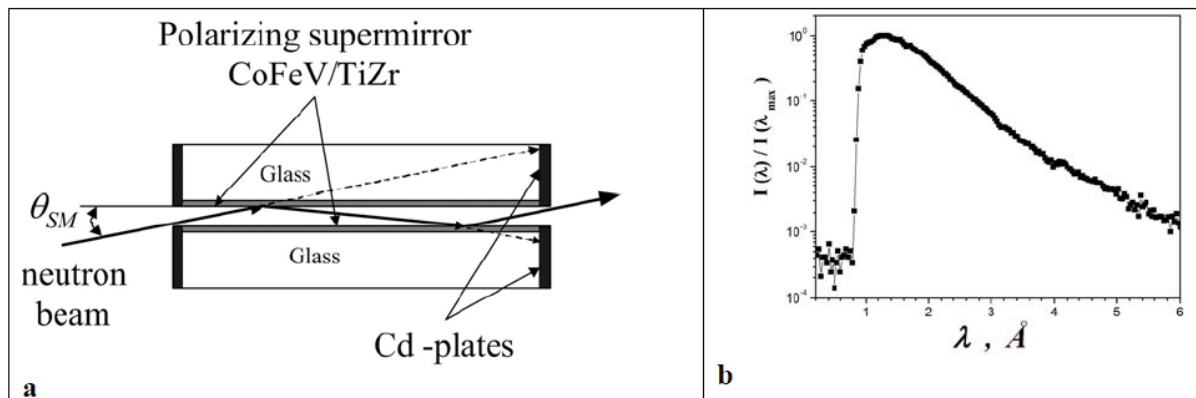


Figure 9. (a) Scheme of CoFeV / TiZr supermirror neutron polarizer based in the unit of the beamformer of neutron reflectometer NR-4M. (b) Relative intensity (as a function of the wavelength) of (+) spin component of the beam at the exit of the supermirror polarizer after double reflection from the polarizer.

The neutron beam with a broad spectral distribution falls on the *CoFeV/TiZr* supermirror [12] at the glancing angle θ_{SM} . In Fig. 9b, the relative intensity is presented as a function of the neutron wavelength. In the spectral range $\lambda = 0.88 - 4.7 \text{ \AA}$ used in this reflectometer, the polarization is very high. Its average value over the spectrum is 0.99. Formed thereby highly polarizing neutron beam with a wide range of wavelength λ passes through the first collimation system, through the first spin-flipper and falls on the sample at the glancing angle θ . The reflected beam from the sample with intensity $I(\lambda)$, after passing through the second spin-flipper, falls on the supermirror analyzer. The reflected beam from the analyzer is recorded by the detector. In this scheme of the total polarization analysis, four spectral intensities ($I^{++}(\lambda)$, $I^{+-}(\lambda)$, $I^{-+}(\lambda)$, $I^{--}(\lambda)$) are measured during four measurements. Carrying out such measurements for a glancing angle θ of the beam containing neutrons with a wide range of wavelength λ , it is possible to obtain four dependences $I^{++}(Q_z)$, $I^{+-}(Q_z)$, $I^{-+}(Q_z)$, $I^{--}(Q_z)$ (where $Q_z = \frac{4\pi \sin \theta}{\lambda}$) within the total polarization analysis.

We propose the new scheme of the total neutron polarization analysis for the reflectometer, where the above NMB based on multilayer periodic Fe / Co nanostructures is used as a monochromator-polarizer. The new scheme of the total neutron polarization analysis is shown in Fig. 10 for the reflectometer without the spin-flipper before the sample.

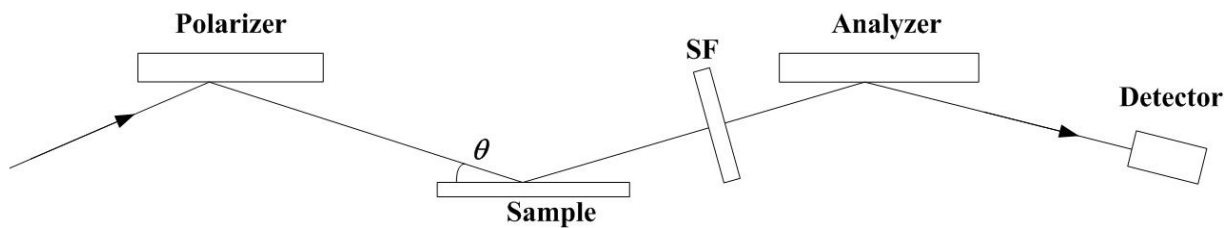


Figure 10. The new scheme of the total neutron polarization analysis for the reflectometer without the spin-flipper before the sample.

There is no spin-flipper before the sample because NMB works as a polarizer in this scheme, which reflects neutrons of both (+) and (-) spin components of the beam. The polarizer is shown in Fig. 11 for the new scheme that is created in the form of the double NMB.

Neutron Double Multimonochromator-Bipolarizer

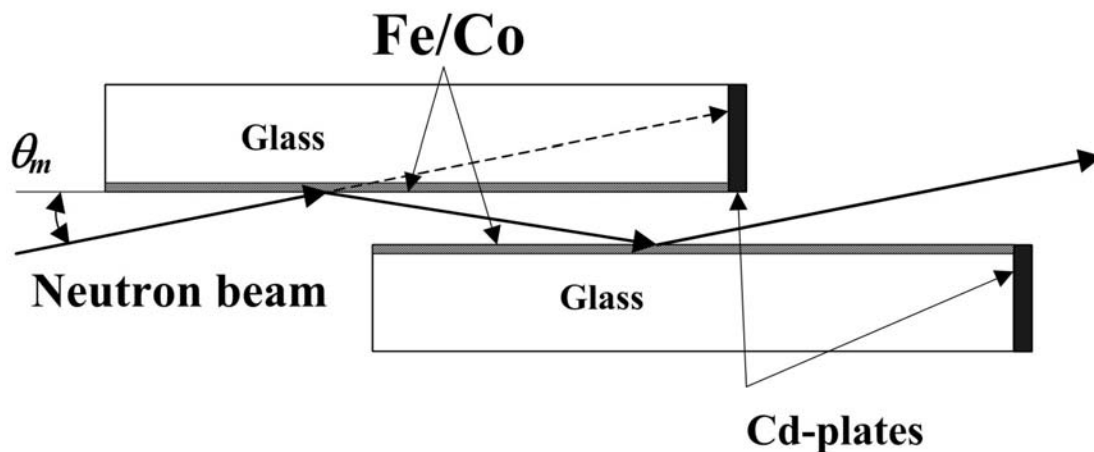


Figure 11. The polarizer for the new scheme of the total neutron polarization analysis for a reflectometer created in the form of the double NMB.

The unpolarized neutron beam with a broad spectral distribution falls on the first mirror of the NMB at angle θ_m . The intensity of the reflected beam shows a set of polarized monochromatic peaks with monotonically growing wavelength. Peaks wavelengths are very close to each other. The neutron polarization is opposite in adjacent peaks. Then, the resulting beam is reflected from the second mirror under the same angle θ_m . The output beam has the same direction, as that falling on the NMB, just as in the cases of Co/Ti monochromator-polarizer and CoFeV/TiZr supermirror considered above. The second reflection allows to make wings of all peaks more sharp. This reduces partial overlapping of wings of the neighboring peaks that allows to increase the polarization of all peaks. At the same time, peaks intensities decrease slightly since reflectivities of peaks are close to 1 (see Table 2). Thus, in this reflectometer, the beam which is twice reflected from NMB and which passes through the collimation system falls on the sample at the glancing angle θ . As it is noted above, it is possible to represent the beam intensity $I(\lambda)$ in the form of the set of monochromatic peaks with monotonically growing

wavelengths. In this set, neighboring peaks have opposite polarizations. As noted above, the use of thirteen pairs of Bragg peaks (Fig. 5) leads to the covering of a large interval of the momentum

transfer $Q_z = 0.043 - 0.131 \text{ \AA}^{-1}$, where $\frac{Q_{z\max}}{Q_{z\min}} \cong 3.05$. Therefore, after reflection of the neutron

beam at angle θ_m from NMB, one obtains the set of 13 pairs of monochromatic peaks. For this set,

the ratio of the maximal wavelength to the minimal one is $\frac{\lambda_{\max}}{\lambda_{\min}} \cong 3.05$, as for the momentum

transfer because $Q_z = \frac{4\pi \sin \theta}{\lambda}$. Bragg peaks of the 3rd order were not considered at the time-of-

flight measurements for all structures except for the structure with period D_{12} . Besides, Bragg peaks of higher orders are not considered as well. Thus, the set of highly polarized monochromatic peaks with opposite polarizations allows to omit the spin-flipper before the sample. Indeed, the intensity of the beam reflected from the sample can be represented in the form of two functions: $I_R^+(\lambda)$ and $I_R^-(\lambda)$ that can be obtained in one measurement. Whereas the conventional scheme requires two measurements at two states of the spin flipper to obtain these functions. The beam reflected from the sample passes through the spin-flipper after the sample, it is then reflected from the analyzer and is registered in the detector. At the same time, we obtain $I_R^{++}(\lambda)$, $I_R^{+-}(\lambda)$ using $I_R^+(\lambda)$ (when the spin-flipper after the sample is switched off) and we find $I_R^{-+}(\lambda)$, $I_R^{--}(\lambda)$ using $I_R^-(\lambda)$ $I_R^+(\lambda)$ (when the spin-flipper after the sample is switched on). Thus, in the new scheme of the total polarization analysis, it is possible to receive four dependences $I_R^{++}(\lambda)$, $I_R^{+-}(\lambda)$, $I_R^{-+}(\lambda)$ and $I_R^{--}(\lambda)$ performing only two measurements. Let us consider the beam reflected from the standard supermirror analyzer for two states of the spin-flipper after the sample (it is switched off (+) and switched on (-)). One obtains $I_R^{++}(\lambda)$ and $I_R^{+-}(\lambda)$ from $I_R^+(\lambda)$ and one obtains $I_R^{-+}(\lambda)$ and $I_R^{--}(\lambda)$ from $I_R^-(\lambda)$. On the other hand, four measurements are required corresponding to four states of two spin-flippers in the case of the traditional total polarization analysis for obtaining four intensities $I_R^{++}(\lambda)$, $I_R^{+-}(\lambda)$, $I_R^{-+}(\lambda)$ and $I_R^{--}(\lambda)$.

4. Discussion and Conclusions

To conclude, we propose the new neutron-optical element - Neutron Multimonomator-Bipolarizer (NMB). It is based on a multimultilayer structure consisting of 12 periodic Fe/Co multilayers which are evaporated on the substrate. The period of these nanostructures increases with distance from the substrate. We present results of calculations of reflectivities of both spin components of a beam from NMB as functions of the momentum transfer.

It is shown that the absorption is quite large of the neutron beam in layers of cobalt during the reflection from the Co/Fe NMB. However, it follows from calculations that the beam attenuation decreases upon decreasing of the number of bilayers. Therefore, it is required to minimize the number of bilayers for each periodic structure of NMB. At the same time, the reflectivity at the Bragg peak of the first order should be close to one. For example, for the structure with the period of 146 Å, the number of bilayers of 245 is apparently almost 8-10 times greater than it is required, because 30-40 bilayers are sufficient for the reflectivity to be close to unity at the Bragg peak of the first order.

We propose the new scheme of the total neutron polarization analysis in reflectometry with

application of double NMB as a polarizer. In this scheme, there is no spin-flipper before the sample. The beam consisting of 13 pairs of monochromatic peaks falls on the sample. Peaks in each pair have opposite polarization. Wavelengths at which peaks arise are close to each other and fill the range

$(\lambda_{\min}, \lambda_{\max})$, where $\frac{\lambda_{\max}}{\lambda_{\min}} \cong 3.05$. Only two measurements are required to find four intensities

$I_R^{++}(\lambda)$, $I_R^{+-}(\lambda)$, $I_R^{-+}(\lambda)$ and $I_R^{--}(\lambda)$.

It is possible to make a compact polarizer based on NMB and to place it at the sample unit in magnetic field. Then, it is possible to remove also the second spin-flipper when using another NMB as the analyzer (instead of the standard supermirror) which is similar to that in the beamformer before the sample. In this case, one can obtain four intensities during two measurements by performing them for two angles of this analyzer which differ from each other by a small angle $\Delta\theta$. Using such a polarizer and such an analyzer, it is possible to create a very compact cell at the sample unit to perform the total polarization analysis without using of spin flippers.

Use of the Neutron Multimonochromator-Bipolarizer is possible in such time-of-flight neutron techniques as polarized neutron reflectometry, SESANS, for research of low-angle and inelastic scattering of polarized neutrons.

Acknowledgements

The work was supported by the Federal target program of Ministry of Education and Science of Russian Federation (project No. RFMEFI61614X0004). Authors are grateful to M. V. Avdeev and Yu. V. Nikitenko for interest in work.

References

- [1] Nikitenko Yu V, Syromyatnikov V G 2013 *Reflectometry of polarized neutrons (M.: Fizmatlit)* 224 p (in russian)
- [2] Schoenborn B P, Caspar D L D, Kammerer O F 1974 *J. Appl. Cryst* **7** 508
- [3] Lynn J W, Kjems J K, Passell L, Saxena A M, Schoenborn B P 1976 *J Appl Cryst* **9** 454
- [4] Saxena A M, Schoenborn B P 1977 *Acta Cryst* **A33** (5) 805
- [5] Gukasov A G, Deriglazov V V, Kezerashvili V Ya, Kudriashov V A, Krutov G A, Peskov B G, Syromyatnikov V G, Trunov V A, Kharchenkov V P, Shchebetov A F 1979 *ZhETF* **77** (5) 1720 (in russian)
- [6] Kezerashvili V Ya, Schebetov A F, Peskov B G, Pleshanov N K, Soroko Z N, Syromyatnikov V G 1987 *Journal of Technical Physics* **57** (7) 1372 (in russian)
- [7] Syromyatnikov V G, Menelle A, Soroko Z N, Schebetov A F 1998 *Physica B* **248** (1–4) 355
- [8] Kyaw Zaw Lin, Syromyatnikov V G 2016 *Vestnik of Saint Petersburg State University series 4* **3** (61) N1 4 (in russian)
- [9] Kyaw Zaw Lin, Syromyatnikov V G 2016 *Journal of Surface Investigation: X-ray, Synchrotron and Neutron Techniques* **10** (4) 687
- [10] Kyaw Zaw Lin, Syromyatnikov V G 2017 *Journal of Surface Investigation: X-ray, Synchrotron and Neutron Techniques* **11** (1) 20
- [11] Syromyatnikov V G et al 2005 *Preprint of Petersburg Nuclear Physics Institute (NRC "Kurchatov Institute")* N 2619 Gatchina 47 p
- [12] Schebetov A F, Pleshanov N K, Syromyatnikov V G et al 1996 *Journal of Physical Society of Japan* **65** supplement A 195